A Simple Algorithm for Increased Helical Pitch in Cone-Beam CT

Michael D. Silver, Katsuyuki Taguchi, Ilmar Hein*

I. INTRODUCTION

A goal of cone-beam CT is to decrease the scan time needed to image a volume of the patient. Four things are required to meet this goal: (1) a detector with multiple rows of sensors, (2) higher bandwidth data acquisition system and image processor to handle the increased data rates and need for fast reconstruction, (3) high helical pitch, (4) a practical reconstruction algorithm that lends itself to fast reconstruction times. Within the last several years, CT-systems with first two, then four row detector arrays have been introduced to the marketplace [1]-[5]. The four row arrays are actually combinations of finer pitched detectors. Table I gives a comparison of the detector designs for the Toshiba Aquilion Multi, the LightSpeed QX/i from General Electric Medical Systems, the Siemens Volume Zoom and Marconi Mx8000. All the major manufacturers have announced plans for an output of 8 and/or 16 slices, which requires a new or modified detector design from Siemens and Marconi. Toshiba has presented images taken on a 256-row prototype detector array [6], [7]. Thus, detector development for wider cone-angles is underway and will lead to faster scan times. The manufacturers are working on the second requirement as computer electronics improve. This presentation looks at the last two requirements. We present a scheme for high helical pitch while maintaining a practical although approximate reconstruction algorithm.

So far, the four row CT-systems have used two-dimensional reconstruction algorithms [8]-[10]. As more rows are added, we have found that three-dimensional backprojection leads to images with better quality than the two-dimensional approximations [11], [12]. Therefore, we believe that as more rows are added to the detector, the reconstruction problem approaches the fully three-dimensional problem. However, because the cone angle is not too large, we propose an approximate algorithm that is a modification of helical Feldkamp [13], [14], where the maximum helical pitch limit is determined by two-dimensional arguments as described in the next section. Moreover, the Feldkamp approach is based on a heuristic use of one-dimensional convolution (rigorous for two-dimensional reconstruction) combined with true three-dimensional backprojection.

We first reported on these ideas at a previous Fully 3D Meeting [15], [16] and presented some results from image evaluation at the last RSNA meeting [17]. Recently [18], we presented how we relate helical pitch, number of views to reconstruct, and field-of-view based on a weighting scheme published in *Medical Physics* [19]. This will be briefly summarized here. In this study, we show how we can extend the maximum helical pitch to higher values.

II. REVIEW: HELICAL, CONE-BEAM SCANNING

A. Validity requirements

Backprojection follows the straight-line ray-sum from the focal spot of the x-ray source through a pixel of interest in the image volume and onto the two-dimensional detector array. Typically, the processed signal at this location in the detector array is weighted and added to the contents of the voxel. This is repeated for all voxels and for a range of x-ray source angles. For helical, cone-beam scanning, the relation between a voxel and a location in the detector array for a given source angle is given by

TABLE I
Comparison of Four-row CT-Scanners

	Toshiba Aquilion Multi	**GE LightSpeed**	**Siemens Volume Zoom Marconi Mx8000**
Detector Rows	34 (4 x 0.5, 30 x 1)	16 (16 x 1.25)	8 (2 x 1, 2 x 1.5, 2 x 2.5, 2 x 5)
DAS Output and nominal slice thicknesses	4 x 0.5, 4 x (1 to 8)	4 x (1.25,2.5,3.75,5)	2 x 0.5, 4 x (1,2.5,5)

Widths of detector rows are given in mm as projected at isocenter. Nominal slice thicknesses are in mm.

$$\gamma(\beta, x, y) = \sin^{-1} \frac{x\cos\beta + y\sin\beta}{L(\beta, x, y)} \tag{1}$$

$$\alpha(\beta, x, y, z) = \tan^{-1} \frac{\left[\beta - \beta_0(z)\right] H}{2\pi L(\beta, x, y)} \tag{2}$$

where γ is the fan angle (in the *x*-*y* plane) of the ray-sum,
α is the cone angle of the ray-sum,
β is the x-ray source angle,
$\beta_0(z)$ is the source angle when the focal spot is in the image slice at *z*,
x,*y*,*z* is the coordinates of an image pixel,
H is the helical pitch: table travel per rotation of the source,

and $L(\beta, x, y) = \sqrt{(R\sin\beta + x)^2 + (R\cos\beta - y)^2}$. (3)

L is the distance from the focal spot to the pixel *x*,*y*,*z* times the cosine of the cone angle, R is the radial distance of the focal spot to isocenter. The coordinate system moves with the patient/table so that each image slice is at a fixed *z*.

Multi-row CT-scanners have detector arrays that are sections of a cylinder, focused on the source; thus equal angular increments $\Delta\gamma$ and equal axial linear increments separate the individual sensor elements. Therefore, γ is a natural coordinate for the ray-sum but (2) is changed in favor of detector rows (also known as slices or segments),

$$n(\beta, x, y, z) = \frac{\left[\beta - \beta_0(z)\right] R}{2\pi L(\beta, x, y)} r_H \,, \tag{4}$$

where n is the relative detector row,

$$-\tfrac{1}{2} \le n \le \tfrac{1}{2} \,, \tag{5}$$

and $$r_H = \frac{H}{W} \tag{6}$$

with W as the full axial height of the detector array as projected at isocenter. Thus, r_H is the normalized helical pitch ratio.

A ray-sum is valid—that is, measured—if γ and n are locations within the physical detector array. For helical, cone-beam CT, the key validity equation is (5) combined with (4). We can solve (4) with $n = \pm\tfrac{1}{2}$ for the surfaces of $\beta_{1,2}$ as a function of voxel position *x*,*y*,*z*; $\beta_{1,2}$ represents the source angular position when the voxel *x*,*y*,*z* enters and then leaves the cone-beam. These surfaces are warped, depending on helical pitch. The difference of the two surfaces shows that up to a normalized helical pitch ratio of 2, all voxels have at least 180° of coverage. Unfortunately, the voxels don't have the same 180° range of coverage. This implies that a reconstruction algorithm could exist that uses only valid ray-sums up to a normalized helical pitch ratio of 2. However, such as algorithm could have additional computational complexities.

B. Weighting Scheme

The helical pitch determines how long a given voxel is irradiated. Obviously, the higher the pitch, the less the voxel is within the rotating cone-beam and vice versa. We adapt the weighting scheme of [19] to helical cone-beam scanning. Consider the sinogram from a single detector row. Suppose all the voxels of a given slice are in the cone-beam for at least $\pi+\Delta\beta$ as shown in Fig. 1a. The weighting scheme, based on Parker's half-scan method [20], introduces a virtual fan-angle, 2Γ, such that $2\Gamma = \Delta\beta$, as shown in Fig. 1b. Use the same weights as in half-scan [20], [21] for the redundant (in two-dimensions) triangles but with 2Γ as the fan-angle.

C. Helical Pitch Limits

Under the condition that we use valid rays-sums, as described in Section II.a, and that all voxels in a slice are reconstructed over the same angular range of the source, then the relation between the angular range of the source used in the reconstruction, the helical pitch, and the field-of-view *FOV* (*R* is the source radius) can be shown to be [17]:

$$\beta_2 - \beta_1 = \pi + 2\Gamma = \frac{2\pi}{r_H} \times \left(1 - \frac{FOV}{2R}\right) \tag{7}$$

The minimum and maximum values for the helical pitch correspond to when the virtual fan-angle approaches π and $2\gamma_m$, the true fan-angle, respectively:

$$r_H(\min, FOV) = 1 - \frac{FOV}{2R} \tag{8}$$

$$r_H(\max, FOV) = \frac{2\pi}{\pi + 2\gamma_m} r_H(\min, FOV) \,. \tag{9}$$

III. INCREASE THE HELICAL PITCH

Keeping the helical pitch below the limit given in (9) assures that all ray-sums that go into making the image are valid ray-sums in a three-dimensional sense, although we use weighting derived from two-dimensional arguments. Consider again Fig. 1b. For the smaller FOV's, the ray-sum values in the region

$$\sin^{-1}\left(\frac{FOV}{2R}\right) < |\gamma| < \gamma_m \tag{10}$$

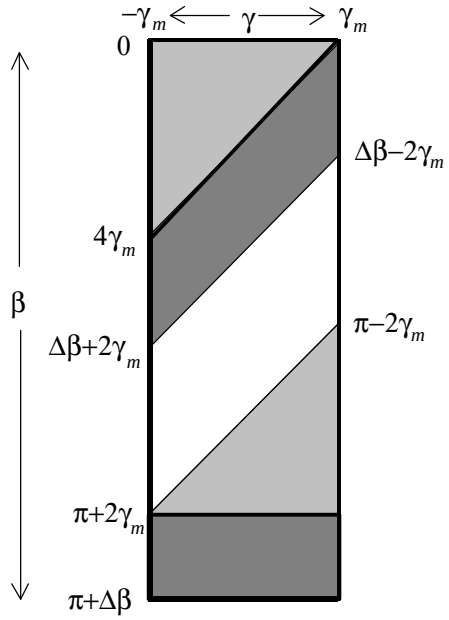

Fig. 1a. Sinogram made from one row of the detector. Similarly shaded regions contain redundant information (ignoring the cone-angle).

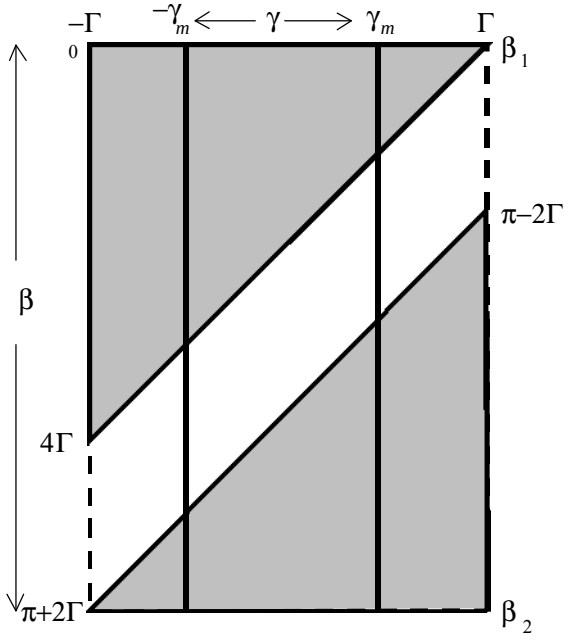

Fig. 1b. Sinogram including two strips of virtual (zeros) data. Fan angle is increased from $2\gamma_m$ to 2Γ. The shaded regions contain redundant information (ignoring the cone angle).

are zero. Note that $\gamma_m = \sin^{-1}\left(\frac{FOV_{\max}}{2R}\right)$, where $FOV_{\max}$ is the maximum field-of-view for the scanner. This implies that the range of validity for (7) is increased. Instead of $r_H(\max, FOV)$ being given by when the virtual fan-angle reaches $2\gamma_m$, it is given by when the virtual fan-angle reaches $2\sin^{-1}\left(\frac{FOV}{2R}\right)$. Therefore, (9) becomes

$$r'_H(\max, FOV) = \frac{2\pi}{\pi + 2\sin^{-1}\left(\frac{FOV}{2R}\right)} r_H(\min, FOV). \quad (11)$$

The ratio of the increase is

$$\frac{r'_H(\max, FOV)}{r_H(\max, FOV)} = \frac{\pi + 2\sin^{-1}\left(\frac{FOV_{\max}}{2R}\right)}{\pi + 2\sin^{-1}\left(\frac{FOV}{2R}\right)}. \quad (12)$$

Fig. 2 compares the new maximum for the helical pitch with the previous calculation as a function of *FOV*. We demonstrate the efficacy of the higher helical pitch with a computer simulation of a 16-row cone-beam CT-scanner using clinical images.

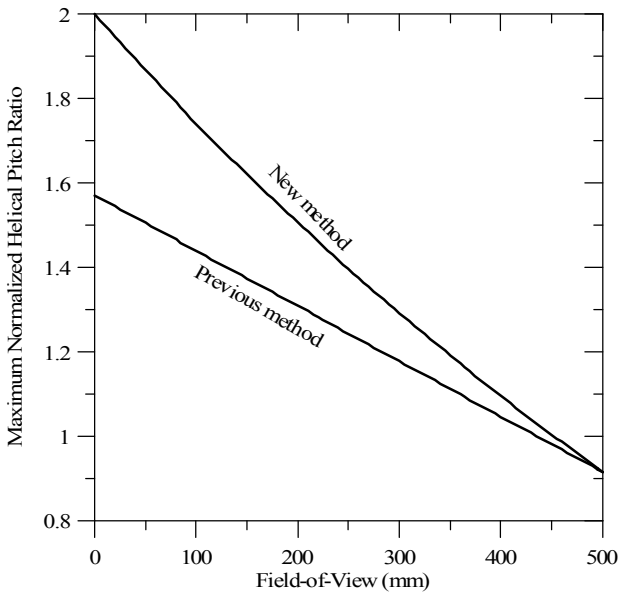

Fig. 2. Maximum helical pitch as a function of *FOV*. Both curves require valid ray-sums and a simple reconstruction algorithm. The previous method uses (9) while the new method uses (11). The curves assume a source radius of 600 mm, a maximum *FOV* of 500 mm.

REFERENCES

[1] Y. Liang and R. A. Kruger, "Dual-slice spiral versus single-slice spiral scanning: comparison of the physical performance of two computed tomography scanners," *Med. Phys.* **23**, 205 – 220 (1996).

[2] C. N. McCollough and F. E. Zink, "Performance evaluation of a multi-slice CT system," *Med. Phys.* **26**, 2223 – 2230 (1999).

[3] H. Hu, H. D. He, W. D. Foley, S. Fox, "Four multidetector-row helical CT: image quality and volume coverage speed," *Radiology*, **215**, 55 – 62 (2000).

[4] W. A. Kalender and T. O. J. Fuchs, "Principles and performance of single-and multi-slice spiral CT," in L. W. Goldman, J. B. Fowlkes, eds., *Categorical Course in Diagnostic Radiology Physics: CT and US Cross-sectional Imaging,* 127 – 142, RSNA, Oakbrook, IL, 2000.

[5] W. A. Kalender, *Computed Tomography*, Publicis MCD Verlag, Munich, 2000.

[6] Y. Saito, H. Aradate, H. Miyazaki, K. Igarashi, H. Ide, "Development of a large area two-dimensional detector for real-time 3-dimensional CT (4D CT)," *Radiology,* **217(p)**, 405 (2000).

[7] Y. Saito, H. Aradate, H. Miyazaki, K. Igarashi, H. Ide, "Large area two-dimensional detector system for real-time three-dimensional CT (4D CT)," *Proc. SPIE*, **4320** (2001).

[8] K. Taguchi and H. Aradate, "Algorithm for image reconstruction in multi-slice helical CT," *Med. Phys.* **25**, 550 – 561 (1998).

[9] H. Hu, "Multi-slice helical CT: Scan and reconstruction," *Med. Phys.* **26**, 5-8 (1999).

[10] S. Schaller, T. Flohr, K. Klingenbeck, J. Krause, T. Fuchs, and W. A. Kalender, "Spiral interpolation algorithm for multi-slice spiral CT – Part I: Theory," *IEEE Trans. Med. Img.* **19**, 822 – 930 (2000).

[11] K. Taguchi, S. Saito, M. Silver, I. Hein, I. Mori, "Evaluation of image reconstruction methods for 8- and 16-slice helical," submitted to *RSNA* 2001.

[12] I. Mori, S. Saito, M. Silver, I. Hein, K. Taguchi, "Eight-slice and 16-slice helical CT: Comparison of image reconstruction methods," submitted to *RSNA* 2001.

[13] L. A. Feldkamp, L. C. Davis, and J. W. Kress, "Practical cone-beam algorithm," *J. Opt. Soc. Am. A,* **1**, 612 – 619 (1984).

[14] H. Kudo and T. Saito, "Three-dimensional helical-scan computed tomography using cone-beam projections," *J. Electron. Information Commun. Soc. Japan,* **J74-D-II**, 1108 – 1114 (1991).

[15] M. D. Silver, "Practical limits to high helical pitch, cone-beam computed tomography," *Proc. 1997 Int. Meeting on Fully 3D Image Reconstruction in Radiology and Nuclear Medicine,* 44-47 (1997).

[16] M. D. Silver, "High-helical-pitch, cone-beam computed tomography," *Phys. Med. Biol.,* **43**, 847 – 855 (1998).

[17] M. D. Silver and K. S. Han, "Application of a new half-scan reconstruction method to helical multi-slice CT (MSCT)," *Radiology,* **217(p)**, 565 (2000).

[18] M. D. Silver, K. Taguchi, and K. Han, "Field-of-view dependent helical pitch in multi-slice CT," *Proc. SPIE*, **4320** (2001).

[19] M. D. Silver, "A method for including redundant data in computed tomography," *Med. Phys.,* **27**, 773 – 774 (2000).

[20] D. L. Parker, "Optimal short scan convolution reconstruction for fan beam CT," *Med. Phys.,* **9**, 254 – 257 (1982).

[21] C. R. Crawford and K. F. King, "Computed tomography scanning with simultaneous patient translation," *Med. Phys.,* **17**, 967 – 982 (1990).

* Michael D. Silver and Ilmar Hein are with Bio-Imaging Research, 425 Barclay Blvd., Lincolnshire, IL 60062, USA (telephone: 847-634-6425, e-mail: msilver@birinc.com and ihein@birinc.com).

Katsuyuki Taguchi is with Medical Systems Company, Toshiba Corporation, Otawara, Tochigi 324-8550, Japan (telephone +81-287-26-6471, e-mail: ktaguchi@mel.nasu.toshiba.co.jp).